

## An Intercalate Molecular Complex of Syndiotactic Polystyrene

Vittorio Petraccone,<sup>\*,†</sup> Oreste Tarallo,<sup>†</sup> Vincenzo Venditto,<sup>‡</sup> and Gaetano Guerra<sup>‡</sup>

Dipartimento di Chimica, Università di Napoli "Federico II", Complesso di Monte S. Angelo, Via Cintia, 80126 Napoli, Italy, and Dipartimento di Chimica, Università di Salerno, I-84081 Baronissi (SA), Italy

Received May 26, 2005; Revised Manuscript Received June 10, 2005

**ABSTRACT:** The crystal structure of the molecular complex of syndiotactic polystyrene (s-PS) with bicyclo[2.2.1]hepta-2,5-diene (norbornadiene, NB) is presented. In analogy to the already described s-PS molecular complexes, this structure presents a monoclinic unit cell (cell constants  $a = 17.5$  Å,  $b = 14.5$  Å,  $c = 7.8$  Å, and  $\gamma = 107.8^\circ$ ) in which the  $s(2/1)2$  polymer helices and guest molecules are packed according to the space group  $P2_1/a$ . However, the structure of the s-PS/NB complex presents layers of contiguous guest molecules alternated with layers of enantiomorphous polymer helices and hence can be described as an intercalate phase. On the other hand, all the known structures of other s-PS molecular complexes present isolated molecules (or a couple of small molecules) into the cavities typical of the nanoporous s-PS  $\delta$  form and hence can be described as clathrate phases. The molar ratio between the monomeric unit and the guest is 2/1 for the s-PS/NB intercalate phase, while it is generally 4/1 for the s-PS clathrate phases.

## Introduction

Syndiotactic polystyrene (s-PS) shows the interesting property to cocrystallize with several low molecular weight substances to form polymer–solvent complexes.<sup>1–6</sup> Up to now, the crystal structures of the s-PS complexes with toluene,<sup>2</sup> iodine,<sup>3</sup> 1,2-dichloroethane,<sup>4</sup> CS<sub>2</sub>,<sup>5</sup> and *o*-dichlorobenzene<sup>6</sup> have been completely characterized. By removal of the guest molecules from all s-PS molecular complexes, it is possible to obtain the nanoporous  $\delta$  form, whose crystal structure has been resolved, too.<sup>7</sup> This form is a nanoporous metastable polymorph of s-PS that is able to rapidly absorb selectively some organic substances from various environments, also when present at low concentration, producing crystalline molecular complexes. For this reason, its employment in the field of molecular sieves for the purification of water or gases<sup>8</sup> or as the sensing film of molecular sensors<sup>9</sup> has been proposed.

The crystal structures of these molecular complexes<sup>2–6</sup> and of the  $\delta$  form<sup>7a</sup> present several common features: (i)  $s(2/1)2$  s-PS helices with a repetition period of 7.7–7.8 Å; (ii) a very efficient close packing of enantiomorphous helices in the  $ac$  plane; (iii) a monoclinic  $P2_1/a$  symmetry; (iv) the presence of isolated centrosymmetric guest locations (which become centrosymmetric cavities for the  $\delta$  form) cooperatively generated by two enantiomorphous helices of two adjacent polymer layers.

The above feature (iv) has allowed to describe all the known s-PS molecular complexes as clathrate phases, since the polymer host forms a cage structure imprisoning the guest. From the comparative study of the crystal structures of the  $\delta$  form and of the known clathrates of s-PS, it can be concluded that, in the process of formation of the clathrates, the  $\delta$  form has the capability to adapt itself to the guest molecule requirements. This process can be described mainly by a shift, along the  $a$  axis direction, of the  $ac$  layers of chains delimiting the cavities, and by an increase of the spacing ( $d_{010} = b \sin$

$\gamma$ ) of the same layers, while the  $a$  axis remains practically constant.<sup>6</sup>

Finally, it is worth noting that up to now it has been found that each cavity hosts just one guest molecule, arranged approximately at its center, thus leading to a maximum molar ratio between polymer monomeric units and guest molecules equal to 4.<sup>2,4,6</sup> The cases of I<sub>2</sub><sup>3</sup> and CS<sub>2</sub><sup>5</sup> clathrate forms, which can host up to two guest molecules per cavity, do not have to be considered exceptions since they present a molecular volume of about one-half of the estimated volume of the  $\delta$  form cavities.<sup>7b,10</sup>

Several clathrate structures have been described also for syndiotactic poly(*p*-methylstyrene) (s-PPMS) in which the polymer chains assume a  $s(2/1)2$  helical conformation similar to that found in the case of s-PS and with the same repetition period.<sup>11,12</sup> At variance with s-PS the behavior of s-PPMS in the formation of clathrates is much more complex. In particular, depending on the shape and the dimensions of the guest molecule, s-PPMS cocrystallizes in clathrate structures characterized by two completely different guest locations: bulky molecules (like *o*-dichlorobenzene<sup>11b</sup>) induce the formation of centrosymmetric guest locations generated by two enantiomorphous adjacent polymer chains very similar to those observed in the already described clathrate forms of s-PS, while small molecules (like tetrahydrofuran<sup>11a</sup>) promote the formation of a second type of guest location, delimited by isomorphous chains related by a  $2_1$  screw axis. In this last case the guest locations are not isolated, and the guest molecules could interact along the  $c$  direction. To differentiate these two types of clathrates, the terms  $\alpha$  class and  $\beta$  class have been introduced, respectively.<sup>11d</sup> According to this nomenclature, all the known clathrate forms of s-PS can be classified as belonging to  $\alpha$  class.<sup>12</sup>

In this paper we present the crystal structure of the molecular complex of s-PS with bicyclo[2.2.1]hepta-2,5-diene (norbornadiene, NB). The main interest to this complex is related to its possible use for molecular size marks of optical data storage systems.<sup>13</sup> In fact, it has been recently described that the valence photoisomerization of NB to quadricyclane, in the crystalline phase,

<sup>†</sup> Università di Napoli "Federico II".

<sup>‡</sup> Università di Salerno.

\* Corresponding author. E-mail: petraccone@chemistry.unina.it.

can occur maintaining for the product quadricyclane the positional and orientational order of the reactant NB, with respect to the polymeric crystallographic axes.<sup>13</sup>

The present structural study is also justified by the unusually low  $2\theta$  value for the lowest diffraction peak ( $<7^\circ$ , corresponding to a Bragg distance of  $d > 13 \text{ \AA}$ )<sup>13</sup> observed for the s-PS/NB molecular complex samples, which anticipated the occurrence of some unusual structural feature.

## Experimental Part and Calculation Methods

**Materials.** Norbornadiene was purchased from Aldrich and used without further purification.

Syndiotactic polystyrene was supplied by Dow Chemical under the trademark Questa 101. <sup>13</sup>C nuclear magnetic resonance characterization showed that the content of syndiotactic polystyrene triads was over 98%. The weight-average molar mass obtained by gel permeation chromatography (GPC) in trichlorobenzene at 135 °C was found to be  $M_w = 3.2 \times 10^5$  with the polydispersity index,  $M_w/M_n = 3.9$ .

Uniaxially oriented amorphous films, 20–40  $\mu\text{m}$  thick, have been obtained by monoaxial stretching of the extruded ones, at draw ratio  $\lambda \approx 3$ , at constant deformation rate of  $0.1 \text{ s}^{-1}$ , in the temperature range 105–110 °C with a Bruker stretching machine. Uniaxially oriented films, presenting the s-PS/NB phase, have been obtained from oriented amorphous films, by exposure to NB vapors at room temperature. The powder presenting the s-PS/NB phase has been obtained by treatment of a  $\delta$  form powder by NB vapor at room temperature. Films presenting the 010 uniplanar orientation of the s-PS/NB phase have been obtained by casting from 5 wt % polymer solution in NB. Before X-ray diffraction measurements, all samples were left at room temperature in air at least for 10 days.

The content of NB molecules was determined by thermogravimetric analysis (TGA) and for the samples which have been used for the X-ray diffraction measurements, was in the range 13–15 wt %.

The molecular volume of the guest molecules has been simply evaluated from their molar mass ( $M$ ) and density ( $\rho$ ):

$$V_{\text{guest}} = M/\rho N_A$$

where  $N_A$  is Avogadro's number ( $6.02 \times 10^{23}$  molecules/mol).

**X-ray Diffraction Measurements.** The X-ray fiber diffraction patterns of oriented samples were obtained on a BAS-MS imaging plate (FUJIFILM) with a cylindrical camera (radius 57.3 mm, Ni-filtered Cu K $\alpha$  radiation monochromatized with a graphite crystal) and processed with a digital scanner (FUJI-BAS 1800).

Wide-angle X-ray diffraction powder patterns were obtained, in reflection with nickel-filtered Cu K $\alpha$  radiation, with an automatic Bruker D8 Advance diffractometer.

Calculated structure factors were obtained as  $F_{\text{calc}} = (\sum |F_i|^2 M_i)^{1/2}$ , where  $M_i$  is the multiplicity factor and the summation is taken over all reflections included in the  $2\theta$  range of the corresponding spot observed in the X-ray fiber diffraction pattern. A thermal factor ( $B = 8 \text{ \AA}^2$ ) and atomic scattering factors from ref 14 were used. The observed structure factors  $F_{\text{obs}}$  were evaluated from the intensities of the reflections observed in the X-ray fiber diffraction pattern ( $I_{\text{obs}}$ ) as  $F_{\text{obs}} = (I_{\text{obs}}/Lp)^{1/2}$ , where  $Lp$  is the Lorentz polarization factor for X-ray fiber diffraction:

$$Lp = \left( \frac{0.5(\cos^2 2\theta + \cos^2 2\theta_M)}{1 + \cos^2 2\theta_M} + \frac{0.5(1 + \cos 2\theta_M + \cos^2 2\theta)}{1 + \cos 2\theta_M} \right) / (\sin^2 2\theta - \zeta^2)^{1/2}$$

with  $2\theta_M = 26.6^\circ$  the inclination angle of the monochromator and  $\zeta = \lambda(l/c)$ ,  $l$  and  $c$  being the order of the layer line and the chain axis periodicity, respectively, and  $\lambda$  is the wavelength of the used radiation (1.5418  $\text{\AA}$ ). The observed intensities  $I_{\text{obs}}$

were evaluated integrating the crystalline peaks observed in the X-ray diffraction profiles, read along different layer lines, after the subtraction of the amorphous contribution. Owing to the different shapes of the reflections on the equator and on the first and second layer lines, due to the different dimensions of the lamellar crystals in the direction perpendicular and parallel to the chain axis, different factors have been used to scale the observed and calculated structure factors on the diverse layer lines. The discrepancy factor  $R$  has been evaluated as

$$R = \sum |F_{\text{obs}} - F_{\text{calc}}| / \sum F_{\text{obs}}$$

taking into account only the observed reflections.

Energy calculations were carried out by using commercially available software (Cerius<sup>2</sup> version 4.2 by Accelrys Inc.). The force field used was the COMPASS force field.<sup>15</sup> The energy was minimized using the Open Force Field module by the smart minimizer method with standard convergence. The starting conformation of the s-PS polymer chains corresponds to that found by molecular mechanics calculations reported in the literature.<sup>16</sup> Since the value of the  $a$  axis of the unit cell is almost identical to those found for all the clathrate structure of this polymer described so far, all the starting models were characterized by an orientation of the polymer chains along the  $a$  axis direction similar to that found for those clathrates, while the independent guest molecule was placed in the space between the  $ac$  layers of chains by trial procedure.

**Infrared Spectroscopy.** Infrared spectra were obtained at a resolution of  $2.0 \text{ cm}^{-1}$  with a Vector 22 Bruker spectrometer equipped with deuterated triglycine sulfate (DTGS) detector and a Ge/KBr beam splitter. The frequency scale was internally calibrated to  $0.01 \text{ cm}^{-1}$  using a He–Ne laser. 32 scans were signal averaged to reduce the noise. Polarized infrared spectra were recorded by use of a SPECAC 12000 wire grid polarizer.

As usual, for each infrared peak an order parameter  $S$  can be defined as the ratio

$$S = (R - 1)/(R + 2)$$

where  $R = A_{\parallel}/A_{\perp}$  is the dichroic ratio,  $A_{\parallel}$  and  $A_{\perp}$  being the measured absorbance for electric vectors parallel and perpendicular to the draw direction, respectively.

The degree of crystallinity has been evaluated by the Fourier transform infrared (FTIR) spectral subtraction procedure described in ref 17.

## Results

**X-ray Diffraction Data.** The X-ray fiber diffraction pattern of a uniaxially oriented film presenting the s-PS/NB molecular complex phase is reported in Figure 1. All the reflections observed in the fiber diffraction pattern are listed in Table 1.

A feature of the X-ray diffraction pattern of the s-PS/NB complex, being unusual for s-PS complexes, is the very low value ( $2\theta = 6.6^\circ$ ) observed for the first peak (Figure 1 and Table 1). This unusual feature can be easily observed also for s-PS/NB complexes presenting different kinds of crystalline phase orientations. Just as an example, the X-ray diffraction patterns obtained by an automatic diffractometer for s-PS/NB complexes, being unoriented (powder) or presenting the (010) uniplanar orientation,<sup>13</sup> clearly show the first diffraction peak located at  $2\theta = 6.5^\circ$  (Figure 2).

In this respect it is worth noting that, for several dozen of s-PS molecular complexes with different guests<sup>18</sup> (e.g., beside the already cited clathrate phases with toluene,<sup>2</sup> iodine,<sup>3</sup> 1,2-dichloroethane,<sup>4,7b</sup> carbon disulfide,<sup>5</sup> *o*-dichlorobenzene,<sup>6</sup> also those including as guest hexane,<sup>18a,b</sup> heptane,<sup>18a,b</sup> cyclohexane,<sup>18l</sup> benzene,<sup>18c</sup> *o*-xylene,<sup>18d</sup> *m*-xylene,<sup>8e</sup> *p*-xylene,<sup>8e</sup> styrene,<sup>18e</sup>



**Figure 1.** X-ray fiber diffraction pattern of a uniaxially stretched film presenting the s-PS/NB molecular complex phase.

**Table 1. Diffraction Angles ( $2\theta_{\text{obs}}$ ), Bragg Distances ( $d_{\text{obs}}$ ), and Intensities ( $I_{\text{obs}}$ ) in Arbitrary Units (AU) of the Reflections Observed on the Layer Lines ( $l$ ) of the X-ray Fiber Diffraction Pattern of the s-PS/NB Film of Figure 1**

$l$	$2\theta_{\text{obs}}$ (deg)	$d_{\text{obs}}$ (Å)	$I_{\text{obs}}$ (AU)
0	6.6	13.4	8700
0	10.65	8.31	6210
0	14.00	6.35	577
0	19.15	4.63	12610
0	24.05	3.70	597
0	31.30	2.86	583
1	14.82	5.98	4849
1	16.64 (broad)	5.33	18422
1	19.56	4.54	15487
1	23.55	3.78	5480
2	24.72 (broad)	3.60	3054
2	28.30	3.15	2660
2	30.50	2.93	834
2	33.48	2.68	268
2	36.52	2.46	259

*p*-methylstyrene,<sup>18l</sup> indene,<sup>18l</sup> naphthalene,<sup>18f</sup> methylene chloride,<sup>1a,18g</sup> chloroform,<sup>8a</sup> chloropropane,<sup>18h</sup> 1,2-dichloropropane,<sup>18h</sup> trichloroethylene,<sup>18i</sup> trichlorobenzene,<sup>18l</sup> *p*-chlorotoluene,<sup>18j</sup> *p*-chlorostyrene,<sup>18k</sup> tetrahydrofuran,<sup>18c</sup> etc.), the first diffraction peak is always in the range 8.37°–7.4° and can be rationalized in terms of a distance between *ac* layers of helices ( $d_{010}$ ) in the range 10.5–12 Å.

This is more clearly pointed out by plotting, for s-PS molecular complexes with different guests, the distance between *ac* layers of helices ( $d_{010}$ ) vs the molecular volume of the guest (Figure 3). It is clearly apparent that, as the volume of the guest molecules increases up to  $\approx 120$  Å<sup>3</sup> (i.e., the estimated volume of the cavity of the  $\delta$  phase),<sup>7b</sup> the  $d_{010}$  value remains close to that one of the empty  $\delta$  phase (10.6 Å). As the volume of the guest molecules increases from 120 Å<sup>3</sup>, a progressive increase of the  $d_{010}$  value up to nearly 12 Å is observed.

Already on inspection of Figure 3, it is apparent that the experimental point corresponding to the s-PS/NB molecular complex (asterisk in Figure 3) is quite far from the generally observed behavior. This clearly suggests that the structure of the s-PS/NB molecular complex has to present structural features definitely

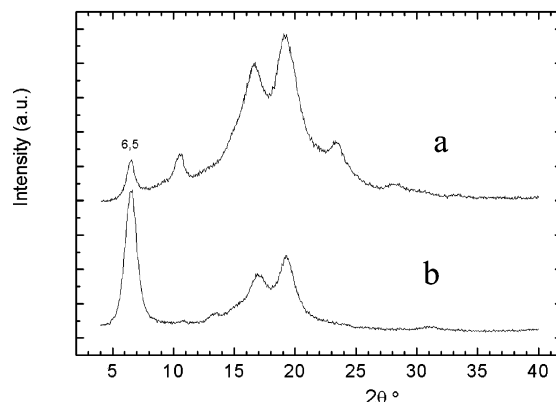


**Figure 2.** X-ray diffraction patterns obtained by an automatic diffractometer for s-PS semicrystalline samples presenting the s-PS/NB crystalline phase: (a) unoriented powder; (b) film presenting the (010) uniplanar orientation of the crystalline phase.

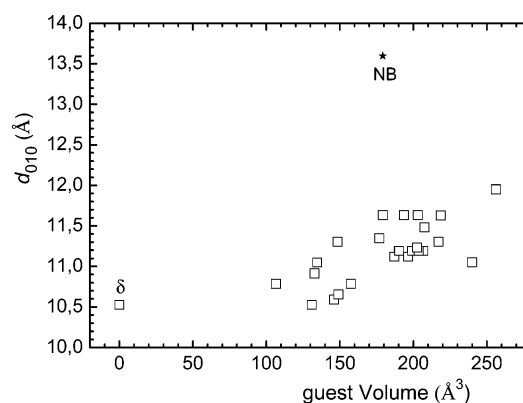


**Figure 3.** Distance between *ac* layers of helices ( $d_{010}$ ) for s-PS molecular complexes with different guests vs the guest molecular volume.

different from those of all other known s-PS molecular complexes.

**Infrared Dichroism Measurements.** Because of the possible presence of guest molecules in both crystalline and amorphous phases, simple thermogravimetric analyses do not give direct information on the host/guest molar ratio in the clathrate phase. This information can be obtained by combining thermogravimetric analyses with infrared dichroism measurements on uniaxially oriented samples.

The NB desorption kinetics, after 7 days of absorption by a uniaxially stretched  $\delta$  form film at room temperature, as evaluated by the FTIR peak absorbances and thermogravimetric measurement (for the plateau value), is reported in Figure 4 (left scale). The initial NB content in the film is higher than 25 wt %, and after a relatively fast desorption rate, it decreases to values in the range 15–10 wt %. In this respect, it is worth adding that the NB uptake from the amorphous phases of s-PS films presenting different crystalline phases ( $\alpha$ ,  $\beta$ , or  $\gamma$ ) is nearly negligible (lower than 1 and 5 wt %, after 7 days of NB sorption at 25 and 60 °C, respectively).

For uniaxially oriented s-PS films with a molecular complex phase, FTIR spectra taken with polarization plane parallel and perpendicular to the draw direction show that most peaks of the considered guest molecules present high dichroic ratios ( $R = A_{\parallel}/A_{\perp}$ ).<sup>18f,19</sup> This clearly indicates that, when included into the crystalline molecular complex, guest molecules present some orientational order with respect to the draw direction.<sup>18f,19</sup>



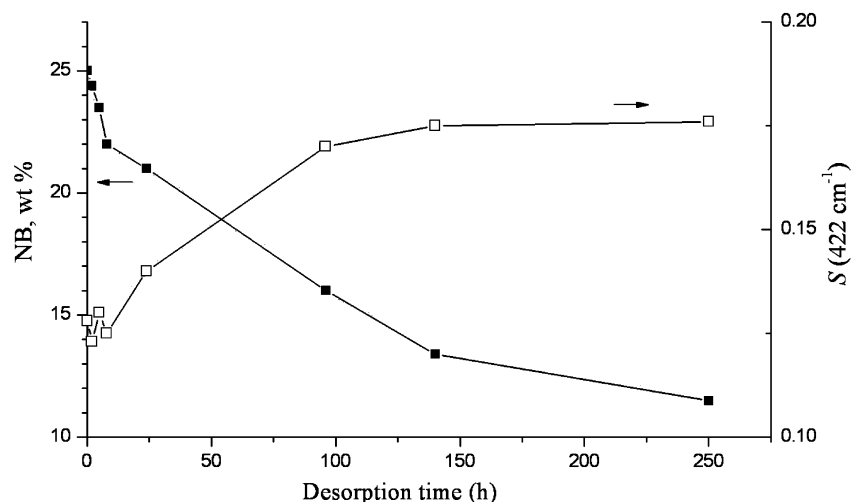


**Figure 4.** NB desorption kinetics (■, left scale) at room temperature, following sorption from a  $\delta$  form uniaxially stretched s-PS film. The order parameter  $S$  obtained from the linear dichroism of the NB  $422\text{ cm}^{-1}$  peak (□, right scale) markedly increases with the desorption time.

On the other hand, the same molecules when absorbed in the amorphous phase are substantially unoriented.<sup>19</sup> As a consequence, the measured dichroic ratios strongly depend on the partition of the guest molecules between the two phases. As discussed in detail in previous papers,<sup>18f,19</sup> after sorption into semicrystalline nanoporous samples, guest molecules can be partitioned almost evenly in amorphous and crystalline phases, but the amorphous phase generally loses the guest molecules at a much faster rate than does the crystalline one and after substantial desorption, most of the residual low molecular weight molecules are located in the crystalline phase. As a consequence, the order parameter ( $S = (R - 1)/(R + 2)$ ) of the guest peaks tend to increase (in absolute value) with guest desorption, gradually reaching a plateau value.

The order parameter  $S$  relative to an intense and isolated peak of NB (at  $422\text{ cm}^{-1}$ , on the right scale) for the s-PS/NB film of Figure 4 is reported on the right scale. It is clearly apparent that the order parameter  $S$  increases with the desorption time, and a plateau value (i.e., a maximum value of dichroism of the guest peak) is reached for norbornadiene content of nearly 14 wt %. In the assumption that, when the  $S$  plateau value is reached, most guest molecules are in the crystalline phase, and on the basis of FTIR evaluated degrees of crystallinity (nearly 35%), it is possible to get approximate estimates of the molar ratio between monomeric unit host/guest molecule, resulting to be nearly 2/1 for the s-PS/NB complex, i.e., quite far from the molar ratio 4/1 typical of s-PS clathrate phases (e.g., with toluene, 1,2-dichloroethane, *o*-dichlorobenzene). It is worth recalling that the molar ratio 2/1 was until now observed only for s-PS clathrates with very small molecules, like  $\text{I}_2$  and  $\text{CS}_2$ , whose volume ( $\approx 60\text{ \AA}^3$ ) is roughly one-half of the volume of the crystalline cavity of the  $\delta$  phase.

The occurrence for the s-PS/NB molecular complex of a molar ratio 2/1 completely different from those observed for s-PS clathrate phases with guest molecules with comparable volumes anticipates (as the considerations on the  $d_{010}$  spacings of the previous section) that the s-PS/NB structure has to present a packing definitely different from those of all other known s-PS molecular complexes.

**Determination of the Crystal Structure.** The reflections of Figure 1 and Table 1 can be indexed in terms of a monoclinic cell with constants  $a = 17.5\text{ \AA}$ ,  $b = 14.5\text{ \AA}$ ,  $c = 7.8\text{ \AA}$ , and  $\gamma = 107.8^\circ$ . The space group is  $P2_1/a$ , in agreement with the systematic absence of  $h k 0$  reflections with  $h = 2n + 1$  and  $00l$  reflections with  $l = 2n + 1$ .

First of all, it is worth noting that the molar ratio 4 between monomeric units and guest molecules, usually observed for guest molecules bulkier than  $\text{I}_2$  or  $\text{CS}_2$ , is inappropriate for this structure since it would lead to a unrealistic calculated density ( $0.88\text{ g/cm}^3$ ) much lower than for the metastable nanoporous  $\delta$  phase ( $0.98\text{ g/cm}^3$ ). The big volume of the proposed unit cell is instead appropriate for the molar ratio 2 (independently evaluated by the infrared dichroism measurements of the previous subsection), corresponding to a calculated ( $1.06\text{ g/cm}^3$ ) density not far from the experimental density value ( $\approx 1.05\text{ g/cm}^3$ ).

Consequently, packing energy calculations have been performed according to the space group  $P2_1/a$  considering an asymmetric unit made of 2 monomeric units of s-PS and one guest molecule, keeping the axes of the unit cell constant. The best result was found for the situation represented in Figure 5. The discrepancy factor  $R$  for this model is 13.7%.

The shortest distance between guest molecule and polymer chain in the final packing model is  $3.77\text{ \AA}$ , while all the guest–guest contact distances are greater than  $3.90\text{ \AA}$  and all the distances among atoms belonging to different chains are greater than  $3.97\text{ \AA}$ . The fractional coordinates of an asymmetric unit of the proposed model are listed in Table 2. Table 3 compares the calculated and the observed structure factors.

## Discussion

The s-PS/NB molecular complex is markedly different with respect to all known s-PS molecular complexes,<sup>2–6,18</sup> which generally present isolated guest locations, roughly corresponding to the crystalline cavities of the nanoporous  $\delta$  phase and hence have been defined as clathrate forms. In fact, for the s-PS/NB molecular complex the guest molecules are arranged in layers and each guest molecule is placed at van der Waals distance from other three neighboring guest molecules. In fact, three couples

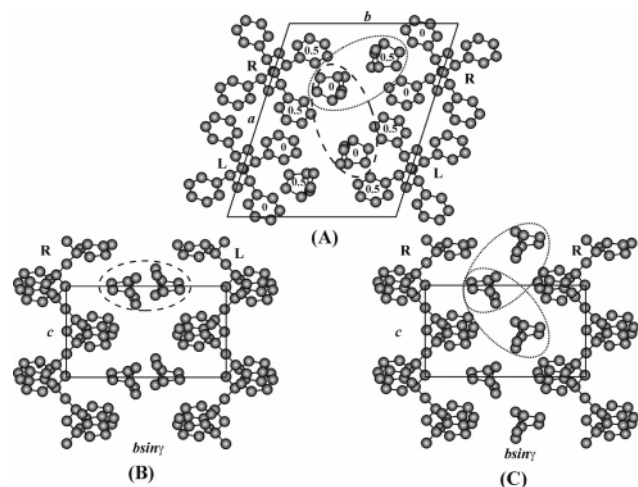


**Figure 5.** Packing model proposed for the crystal structure of s-PS molecular complex containing norbornadiene, in the space group  $P2_1/a$ . In (A) the whole content of the unit cell in the  $ab$  projection is shown while in (B) and (C) the  $cb \sin \gamma$  projections of the packing between only one couple of enantiomorphous (along  $b + a/2$  direction) and only one couple of isomorphous (along  $b$  direction) polymer chains, are shown, respectively. The ellipses indicate couples of neighboring guest molecules at van der Waals distance one from another. Dashed ellipses (A, B) delimit couples arranged similarly to  $\alpha$  class clathrates while dotted ones (A, C) delimit couples arranged similarly to  $\beta$  class clathrates (see discussion in the text for details). The approximate  $z/c$  fractional coordinates of some barycenters of the phenyl rings and of some guest molecules are shown. R = right-handed, L = left-handed helices.

**Table 2. Fractional Coordinates of the Atoms of an Asymmetric Unit of the Model Proposed (Figure 5) for the Molecular Complex of s-PS with Norbornadiene<sup>a</sup>**

	$x/a$	$y/b$	$z/c$
C1	0.153	-0.004	0.251
C2	0.185	-0.066	0.375
C3	0.248	-0.005	0.503
C4	0.115	-0.062	0.630
C5	0.115	-0.134	0.471
C6	0.066	-0.101	0.580
C7	0.002	-0.164	0.667
C8	-0.015	-0.264	0.645
C9	0.033	-0.299	0.536
C10	0.097	-0.234	0.450
C11	0.324	-0.126	0.532
C12	0.388	-0.148	0.420
C13	0.423	-0.249	0.331
C14	0.395	-0.249	0.355
C15	0.331	-0.288	0.468
C16	0.296	-0.227	0.555
C17	-0.147	-0.707	0.038
C18	-0.104	-0.599	0.067
C19	-0.154	-0.563	0.197
C20	-0.225	-0.571	0.125
C21	-0.225	-0.612	-0.056
C22	-0.219	-0.714	-0.034
C23	-0.135	-0.561	-0.095

<sup>a</sup> Hydrogen atoms were included in the structure factors calculation, but they are omitted in this table for simplicity.

of neighboring molecules, sharing a molecule, can be identified (see Figure 5): a first couple (Figure 5B) is arranged as in the case of the clathrate forms of s-PS with  $I_2$  and  $CS_2$  (in which each isolated cavity can host up to two molecules, see Figure 6A);<sup>2,5</sup> the other two couples (Figure 5C) are arranged, instead, as in the s-PPMS  $\beta$  class clathrates (as for the case of the clathrate form of sPPMS containing tetrahydrofuran reported in Figure 6B), since the guests follow one

**Table 3. Comparison between Calculated ( $F_{calc}$ ) and Observed Structure Factors ( $F_{obs}$ ), Evaluated from the Intensities Observed in the X-ray Fiber Diffraction Pattern of Figure 1, for the Model of the Molecular Complex of s-PS with Norbornadiene of Figure 5<sup>a</sup>**

$hkl$	$d_{obs}$ (Å)	$d_{calc}$ (Å)	$F_{calc}$	$F_{obs}$
010	13.4	13.80	70	87
210		8.33	30	84
200	8.31	8.31	78	
220		6.35	2	30
210	6.35	6.32	30	
230		4.67	117	181
220	4.63	4.66	136	
030		4.60	25	42
420		4.17		
400		4.16	31	45
430		3.70	43	
410	3.70	3.68	14	79
250		2.90	60	
620		2.90	8	51
610	2.86	2.89	5	
240		2.89	50	24
450		2.71		
640		2.58	25	24
610		2.57		
260		2.41	32	77
111	5.98	5.98		
121		5.29	156	167
021	5.33	5.17	23	
221		4.92	28	95
211		4.91	47	
311		4.65	92	144
121		4.64		
301	4.54	4.52	144	43
321		4.30	77	
231		4.01		24
311		4.01		
221		4.00	25	108
411		3.81		
331		3.72	22	46
421	3.78	3.68		
401		3.67	50	19
131		3.64		
321		3.41	25	34
141		3.27		
041		3.15	21	24
521		3.14		
141		2.95	39	26
251		2.72		
621		2.71	24	27
611		2.71		
241		2.71	29	23
631		2.62		
641		2.45	25	32
611		2.44		
112		3.73	48	38
112		3.60		
212	3.60	3.53	52	50
202		3.53		
122		3.43	32	51
022		3.39		
312		3.23	27	20
122		3.23		
302	3.15	3.19	61	75
322		3.11		
312		2.99	64	16
222	2.93	2.99		
032		2.97	30	53
422		2.91		
432		2.68	40	42
412		2.68		
142	2.68	2.65	7	12
242		2.64		
232		2.64	16	18
512		2.60		
522		2.58	45	26
502		2.53		
532		2.47	18	11
142		2.47		
442	2.46	2.46	37	41
422		2.45		
333		2.43	9	23
512		2.39		

<sup>a</sup> The Bragg distances ( $d_{obs}$ ), observed in the X-ray fiber diffraction pattern and calculated ( $d_{calc}$ ) for the Proposed Monoclinic Unit Cell ( $a = 17.5$  Å,  $b = 14.5$  Å,  $c = 7.8$  Å, and  $\gamma = 107.8^\circ$ ) are also shown. Reflections not observed with  $F_{calc} < 20$  have not been reported.  $F_{obs}$  reported have been scaled by a factor 3.1 on the equatorial layer line, 2.8 on the first layer line, and 5.3 on the second layer line.

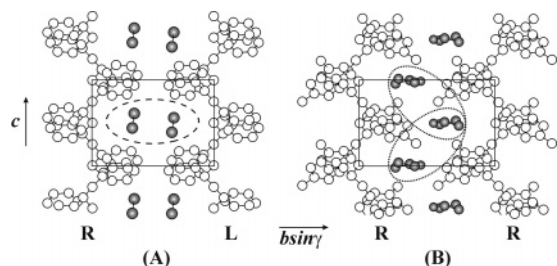


**Figure 6.** Schematic projections in the  $cb \sin \gamma$  plane for the crystal structure of molecular complexes of s-PS containing iodine<sup>3</sup> (A) and s-PPMS with tetrahydrofuran<sup>11a</sup> (B). Only one couple of enantiomorphous (A) and isomorphous (B) polymer chains delimiting the guest locations are shown. R = right-handed, L = left-handed helices. The ellipses indicate "couples" of neighboring guest molecules at van der Waals distance one from another.

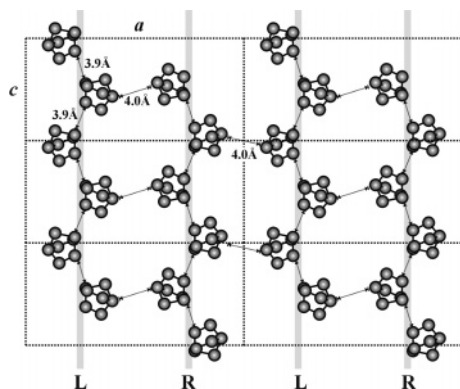


**Figure 7.** Projection along the  $b$  axis of a layer of guest molecules parallel to the  $ac$  layer of chains. Six unit cells are shown. The positions of the chain axis of the polymer chains are indicated by a gray rectangle. The shortest distances between the guest molecules are also indicated. R = right-handed, L = left-handed helices.

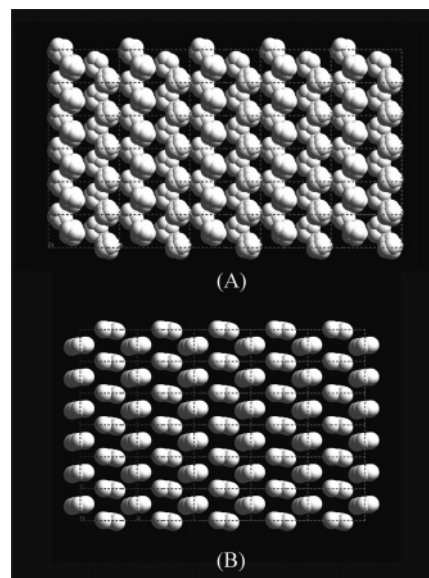
another at van der Waals distance roughly along the polymer chain axis.<sup>11a</sup>

Figure 7 shows the projection along the  $b$  axis of one of these layers of guest molecules which alternate with parallel  $ac$  layers of enantiomorphous helices. Since the guest molecules are not imprisoned into host cavities, this kind of molecular complex cannot be defined a *clathrate* but can be more correctly defined as an *intercalate*.

To compare the arrangement of the guest molecules for this intercalate molecular complex with usual s-PS clathrate molecular complexes, the same kind of projection of Figure 7 is represented in Figure 8 for guest molecules (represented with their van der Waals encumbrance) of the s-PS/NB and s-PS/*o*-dichlorobenzene<sup>6</sup> molecular complexes.

For the s-PS/norbornadiene intercalate complex, the separation between the  $ac$  layers of helices is much larger ( $d_{010} = 13.2 \text{ \AA}$ ) than for the other s-PS clathrate phases ( $d_{010}$  in the range  $10.5\text{--}12 \text{ \AA}$ ). Hence, while for the s-PS clathrates the packing is dominated by the intermolecular interactions between the polymer helices, for the s-PS/NB intercalate these interactions dominates only the packing in the  $ac$  polymer layers while the packing perpendicular to the  $ac$  planes depend as well on polymer/guest and guest/guest interactions.

It is worth adding that, although the NB guest molecules are arranged in layers rather than isolated, their removal from the s-PS/NB clathrate phase, by



**Figure 8.** Comparison between the van der Waals encumbrance of the guest molecules in a projection parallel to the  $ac$  plane, for the molecular complexes of s-PS with norbornadiene (A) and *o*-dichlorobenzene<sup>6</sup> (B).

substitution with volatile guest molecules,<sup>7,18e</sup> leads as usual to the  $\delta$  phase, which presents isolated cavities.<sup>7</sup>

The possible occurrence of intercalate phases for s-PS, analogous to the s-PS/NB molecular complex, could possibly contribute to rationalize diffraction data and phase behaviors of s-PS gels. In fact, it is well-known that the polymer-rich phases of the most stable s-PS gels correspond to crystalline molecular complexes with  $s(2/1)2$  helices.<sup>20</sup> It has been also clearly established that generally the crystalline phases of the s-PS gels are clathrate phases.<sup>20d,e,h,i</sup> However, by neutron diffraction of gels of deuterated s-PS in deuterated benzene, it has been established that while for concentrated gels (57 wt %) the usual diffraction pattern of the s-PS/benzene clathrate phase is present, for diluted gels (26 wt %) a different diffraction pattern, showing an intense low  $2\theta$  peak for  $d \approx 15 \text{ \AA}$ , is observed.<sup>20d</sup> Moreover, the phase diagram study of the s-PS/benzene system has suggested the possible occurrence of two molecular complexes with markedly different stoichiometries.<sup>20d</sup> Low  $2\theta$  peaks corresponding to  $d \approx 15 \text{ \AA}$  have been also observed for s-PS gels in benzyl methacrylate and in cyclohexyl methacrylate.<sup>20f,g</sup> In our opinion, a contribution to the structure determination for these crystalline gel phases could come by considering the possibility of formation of intercalate structures (monomer/guest molar ratio 2) beside the usual clathrate structures (monomer/guest molar ratio 4).

## Conclusions

The crystal structure of the s-PS molecular complex with norbornadiene presents a monoclinic unit cell (cell constants  $a = 17.5 \text{ \AA}$ ,  $b = 14.5 \text{ \AA}$ ,  $c = 7.8 \text{ \AA}$ , and  $\gamma = 107.8^\circ$ ) in which the  $s(2/1)2$  polymer helices and guest molecules are packed according to the space group  $P2_1/a$ .

The packing of the s-PS/NB molecular complex is characterized by  $ac$  layers of enantiomorphous helices alternated with layers of contiguous guest molecules while the packing of the already known s-PS molecular complexes presents isolated guest locations, roughly corresponding to the thoroughly characterized cavities



of the nanoporous  $\delta$  phase.<sup>7</sup> Hence, the s-PS/NB molecular complex can be defined an *intercalate* while the already known s-PS molecular complexes have been defined *clathrates*.

The intercalate complex presents a guest content much higher than the clathrate complexes. In fact, the molar ratio between monomeric units and the NB guest molecules is 2 rather than 4 as usual for clathrates with bulky guest molecules. This unusual molar ratio has been confirmed by independent infrared dichroism measurements combined with thermogravimetric analyses.

It is worth noting that the isolation of the guest molecules in s-PS clathrate phases has precluded the occurrence of their intermolecular reactions (e.g., possible polymerizations of guest monomers). The contiguity between the guest molecules of the s-PS/NB intercalate opens the possibility of intermolecular reactions. In particular, it is worth recalling that norbornadiene is a well-known monomer for radical polymerizations,<sup>21</sup> and hence its layer arrangement could be exploited for a possible solid-state polymerization in the crystalline phase, possibly induced by  $\gamma$  irradiation. These kinds of process could in principle lead to new nanostructured polymeric blends.

**Acknowledgment.** Financial support of the “Ministero dell’Istruzione, dell’Università e della Ricerca” (CLUSTER 26 and PRIN 2004) and of “Regione Campania” (Legge 5 and Centro di Competenza per le Attività Produttive) is gratefully acknowledged. Dr. Concetta D’Aniello is gratefully acknowledged for experimental support and useful discussions.

## References and Notes

- (1) (a) Immirzi, A.; de Candia, F.; Iannelli, P.; Zambelli, A.; Vittoria, V. *Makromol. Chem., Rapid Commun.* **1988**, *9*, 761–764. (b) Vittoria, V.; de Candia, F.; Iannelli, P.; Immirzi, A. *Makromol. Chem., Rapid Commun.* **1988**, *9*, 765–769. (c) Guerra, G.; Vitagliano, M. V.; De Rosa, C.; Petraccone, V.; Corradini, P. *Macromolecules* **1990**, *23*, 1539–1544.
- (2) Chatani, Y.; Shimane, Y.; Inagaki, T.; Iijtsu, T.; Yukimori, T.; Shikuma, H. *Polymer* **1993**, *34*, 1620–1624.
- (3) Chatani, Y.; Inagaki, T.; Shimane, Y.; Shikuma, H. *Polymer* **1993**, *34*, 4841–4845.
- (4) De Rosa, C.; Rizzo, P.; Ruiz de Ballesteros, O.; Petraccone, V.; Guerra, G. *Polymer* **1999**, *40*, 2103–2110.
- (5) Tarallo, O.; Petraccone, V. *Macromol. Chem. Phys.* **2004**, *205*, 1351–1360.
- (6) Tarallo, O.; Petraccone, V. *Macromol. Chem. Phys.* **2005**, *206*, 672–679.
- (7) (a) De Rosa, C.; Guerra, G.; Petraccone, V.; Pirozzi, B. *Macromolecules* **1997**, *30*, 4147–4152. (b) Milano, G.; Venditto, V.; Guerra, G.; Cavallo, L.; Ciambelli, P.; Sannino, D. *Chem. Mater.* **2001**, *13*, 1506–1511.
- (8) (a) Manfredi, C.; Del Nobile, M. A.; Mensitieri, G.; Guerra, G.; Rapacciuolo, M. *J. Polym. Sci., Polym. Phys. Ed.* **1997**, *35*, 133–140. (b) Guerra, G.; Milano, G.; Venditto, V.; Musto, P.; De Rosa, C.; Cavallo, L. *Chem. Mater.* **2000**, *12*, 363–368. (c) Musto, P.; Mensitieri, G.; Cotugno, S.; Guerra, G.; Venditto, V. *Macromolecules* **2002**, *35*, 2296–2304. (d) Sivakumar, M.; Yamamoto, Y.; Amutharani, D.; Tsujita, Y.; Yoshimizu, H.; Kinoshita, T. *Macromol. Rapid Commun.* **2002**, *23*, 77–79. (e) Yamamoto, Y.; Kishi, M.; Amutharani, D.; Sivakumar, M.; Tsujita, Y.; Yoshimizu, H. *Polym. J.* **2003**, *35*, 465–469. (f) Daniel, C.; Alfano, D.; Venditto, V.; Cardea, S.; Reverchon, E.; Larobina, D.; Mensitieri, G.; Guerra, G. *Adv. Mater.* **2005**, *17*, 1515–1518.
- (9) (a) Mensitieri, G.; Venditto, V.; Guerra, G. *Sens. Actuators B* **2003**, *92*, 255–261. (b) Giordano, M.; Russo, M.; Cusano, A.; Cutolo, A.; Mensitieri, G.; Nicolais, L. *Appl. Phys. Lett.* **2004**, *85*, 5349–5351. (c) Arpaia, P.; Guerra, G.; Mensitieri, G.; Schiano Lo Moriello, R. *IEEE Trans. Instrum. Meas.* **2005**, *54*, 31–37.
- (10) Tamai, Y.; Fukuda, M. *Chem. Phys. Lett.* **2003**, *371*, 620–625.
- (11) (a) Petraccone, V.; La Camera, D.; Pirozzi, B.; Rizzo, P.; De Rosa, C. *Macromolecules* **1998**, *31*, 5830–5836. (b) Petraccone, V.; La Camera, D.; Caporaso, L.; De Rosa, C. *Macromolecules* **2000**, *33*, 2610–2615. (c) La Camera, D.; Petraccone, V.; Artimagnella, S.; Ruiz de Ballesteros, O. *Macromolecules* **2001**, *34*, 7762–7766. (d) Dell’Isola, A.; Floridi, G.; Rizzo, P.; Ruiz de Ballesteros, O.; Petraccone, V. *Macromol. Symp.* **1997**, *114*, 243–249.
- (12) Petraccone, V.; Tarallo, O. *Macromol. Symp.* **2004**, *213*, 385–394.
- (13) Stegmaier, P.; De Girolamo Del Mauro, A.; Venditto, V.; Guerra, G. *Adv. Mater.* **2005**, *17*, 1166–1168.
- (14) Cromer, D. T.; Mann, J. B. *Acta Crystallogr.* **1968**, *A24*, 321–324.
- (15) Sun, H. *J. Phys. Chem. B* **1998**, *102*, 7338–7364.
- (16) Corradini, P.; Napolitano, R.; Pirozzi, B. *Eur. Polym. J.* **1990**, *26*, 157–161.
- (17) (a) Daniel, C.; Guerra, G.; Musto, P. *Macromolecules* **2002**, *35*, 2243–2251. (b) Albuñia, A. R.; Musto, P.; Guerra, G., submitted to *Polymer*.
- (18) (a) Guerra, G.; Milano, G.; Venditto, V.; Loffredo, F.; Ruiz de Ballesteros, O.; Cavallo, L.; De Rosa, C. *Makromol. Chem. Phys., Makromol. Symp.* **1999**, *138*, 131–137. (b) Uda, Y.; Kaneko, F.; Kawaguchi, T. *Macromol. Rapid Commun.* **2004**, *25*, 1900–1904. (c) Rizzo, P.; Della Guardia, S.; Guerra, G. *Macromolecules* **2004**, *37*, 8043–8049. (d) Loffredo, F.; Pranzo, A.; Venditto, V.; Longo, P.; Guerra, G. *Macromol. Chem. Phys.* **2003**, *204*, 859–867. (e) Reverchon, E.; Guerra, G.; Venditto, V. *J. Appl. Polym. Sci.* **1999**, *74*, 2077–2082. (f) Venditto, V.; Milano, G.; De Girolamo Del Mauro, A.; Guerra, G.; Mochizuki, J.; Itagaki, H. *Macromolecules* **2005**, *38*, 3696–3702. (g) Bhoje Gowd, E.; Nair, S. S.; Ramesh, C. *Macromolecules* **2002**, *35*, 8509–8514. (h) Musto, P.; Manzari, M.; Guerra, G. *Macromolecules* **2000**, *33*, 143–149. (i) Rizzo, P.; Costabile, A.; Guerra, G. *Macromolecules* **2004**, *37*, 3071–3076. (j) Mahesh, K. P. O.; Sivakumar, M.; Yamamoto, Y.; Tsujita, Y.; Yoshimizu, H.; Okamoto, S. *J. Polym. Sci., Polym. Phys.* **2004**, *42*, 3439–3446. (k) De Girolamo Del Mauro, A.; Loffredo, F.; Venditto, V.; Longo, P.; Guerra, G. *Macromolecules* **2003**, *36*, 7577–7584. (l) Our unpublished data.
- (19) Albuñia, A. R.; Di Masi, S.; Rizzo, P.; Milano, G.; Musto, P.; Guerra, G. *Macromolecules* **2003**, *36*, 8695–8703.
- (20) (a) Kobayashi, M.; Kozasa, T. *Appl. Spectrosc.* **1993**, *9*, 1417–1424. (b) Deberdt, F.; Berghmans, H. *Polymer* **1994**, *35*, 1688–1693. (c) Kobayashi, M.; Yoshioka, T.; Imai, M.; Itoh, Y. *Macromolecules* **1995**, *28*, 7376–7385. (d) Daniel, C.; Deluca, M. D.; Guenet, J. M.; Brulet, A.; Menelle, A. *Polymer* **1996**, *37*, 1273–1280. (e) Daniel, C.; Menelle, A.; Brulet, A.; Guenet, J. M. *Polymer* **1997**, *38*, 4193–4199. (f) Rastogi, S.; Goossens, J. G. P.; Lemstra, P. J. *Macromolecules* **1998**, *31*, 2983–2998. (g) van Hooy-Corstjens, C. S. J.; Magusin, P. C. M. M.; Rastogi, S.; Lemstra, P. J. *Macromolecules* **2002**, *35*, 6630–6637. (h) Daniel, C.; Alfano, D.; Guerra, G.; Musto, P. *Macromolecules* **2003**, *36*, 1713–1716. (i) Daniel, C.; Alfano, D.; Guerra, G.; Musto, P. *Macromolecules* **2003**, *36*, 5742–5750.
- (21) (a) Alupe, V.; Choi, S. W.; Alupe, I. C.; Ritter, H. *Polymer* **2004**, *45*, 2111–2117. (b) Pellon, J.; Kugel, R. L.; Marcus, R.; Rabinowitz, R. *J. Polym. Sci., Part. A* **1964**, *2*, 4105–4112.

MA051075W